Electrical and mechanical properties of ultra-small Au contacts

A. Stalder and U. Dürig
IBM Research Division, Zurich Research Laboratory, CH-8803 Rüschlikon, Switzerland
(September 22, 1994)

Electrical and mechanical properties of point contacts of atomic dimensions have been studied using a scanning tunneling microscope supplemented by a force sensor for measuring tip–sample forces. It is shown that the conductivity and the atomic structure of the contact are intimately related. Measured stress–strain characteristics suggest that plastic deformation proceeds by nucleation of slip dislocations and subsequent shear. The yield strength observed is of the order of 6 GPa which proves that nanometer-sized contacts are substantially more rigid than their macroscopic counterparts.

Metallic contacts are essential to deal with a variety of important practical problems such as adhesion, wear, and friction. Traditionally, contacts have been studied in indentation experiments [1–3]. Spurred by the development of scanning tunneling (STM) and scanning force microscopy, contact experiments have been extended to the nanometer regime [4–6]. Ultimately, point contacts of atomic dimensions can be made; which has been convincingly demonstrated by electrical conductivity measurements [7–9]. A common feature of all these experiments is a jump to contact as the tip approaches the surface. This jump manifests itself as an abrupt increase of the electrical conductivity and of the adhesive force. Upon retraction a neck is formed as a consequence of plastic deformation.

Our present understanding of deformation mechanics on the nanometer scale relies to a large extent on results obtained from molecular dynamics (MD) simulations [10–13]. Basically, the deformation of the neck is predicted to involve a series of subsequent structural transformations between ordered and disordered states. In each transformation cycle the diameter of the neck discontinuously shrinks as an atomic layer is being added. Stress–strain characteristics are predicted to exhibit a characteristic undulation with a period approximately equal to the lattice constant.

Despite long-standing experimental efforts, no measured data of stress–strain characteristics of atomic-scale contacts have been published, nor have periodic oscillations of contact forces been observed. A major difficulty with such experiments is that they are not strictly reproducible. After each indentation–retraction cycle, the tip shape has changed as a result of plastic deformation. Furthermore, the experimental setup is required to be very stiff if measurements are not to be corrupted by a trivial mechanical instability of the apparatus. This has stringent consequences for the force sensor, which must be carefully optimized. With this in mind, an STM-based indentation experiment was set up to explore necking and plastic flow in atomic-scale Au junctions by measuring contact forces and electrical resistance as a function of tip–sample distance.

The experiment was performed under high-vacuum conditions ($p \leq 10^{-6}$ mbar). The apparatus consisted of an STM complemented by a force sensor as sample stage. Thin (≈2000 Å) (111)-oriented Au films evaporated on glass substrates served as samples and electrochemically etched Au wires were used as tips. The tips were conditioned *in situ* by applying short (≈200 ms) pulses of a high positive bias voltage (≈100 V) to the tip during tunneling. The process was stopped when a tunnel barrier height of > 1 eV was measured, and attractive tip–sample forces smaller than a few nanonewtons were observed during tunneling, which can be taken as an indication for a sharp tip.

Simulations suggest that necking of atomic-sized contacts gives rise to negative tip–sample force gradients of the order of $-50\,\mathrm{Nm}^{-1}$ [11,13]. Hence, in order to sustain this adhesive interaction, the stiffness of the force sensor should be larger than, say, $100\,\mathrm{Nm}^{-1}$, which makes it difficult to measure contact forces on a nanonewton scale by means of deflection sensing. Therefore, a force sensor was developed that eliminates the latter [14]. It consists of a cantilever beam (CB), which holds the sample at its free end, and a carbon fiber with a diameter of $5\,\mu$m, which is stretched between the free end of the CB and a miniature piezoelectric friction glider (see Fig. 1). The glider is used for adjusting the tension in the fiber. A force acting between tip and sample causes a deflection of the CB. Accordingly, the tension in the fiber changes, causing its resonance frequency for transverse oscillations to shift. Thus, tip–sample forces can be determined from a simple frequency measurement. For this purpose the string is used as a resonator in a phase-controlled oscillator [15]. The force sensor can be reliably characterized and calibrated (for details see [14]). The stiffness of the sensor in terms of displacements of the sample along the tip axis was $C = 160\,\mathrm{Nm}^{-1}$, and a sensitivity of 0.5 nN for an integration time of 10 ms was achieved.

Tunneling (bias voltage = 10 mV, current = 0.1 nA) was used to establish a well-defined initial tip-sample distance previous to an indentation experiment. The latter consists of ramping the tip forward by ≈30 Å and subsequently retracting it by twice the approach distance at a rate of 10 Ås^{-1}, while simultaneously measuring the tip–sample force and the contact resistance by taking data samples every 10 ms. At the end of one such cycle, the tip is laterally displaced by 100 Å before a new measurement is started. Experimentally the tip excursion, Δz, is the control parameter. To obtain the actual motion of the tip relative to the sample, Δs, one must correct for the response of the force sensor by using the transformation $\Delta s = \Delta z - C\Delta F_{\mathrm{TS}}$, where C is the spring constant of the sensor and ΔF_{TS} denotes the corresponding change of the tip–sample force.

The contact resistance provides a direct measure of the contact area. However, its magnitude varies from GΩ in the tunneling regime to $\approx 100\,\Omega$ for a 100-Å diameter contact. A full characterization of the indentation process therefore calls for a continuous current measurement spanning seven orders of magnitude. This was achieved by using a current-to-voltage converter with a quasilogarithmic transfer characteristic. The converter was carefully calibrated such that relative errors are less than 2% over the entire dynamic range from 10 pA to 10 mA. Moreover, the input impedance was measured to be less than 1 Ω, and can thus be neglected.

A comprehensive description of electron conduction in atomic-sized contacts is obtained if subtleties due to scattering in the conduction channel are neglected. Let us assume that the length of the neck is small compared to the mean free path of electrons, ℓ. Classically, the neck then acts like a two-dimensional aperture whose conductance scales as $1/d^2$ or $1/d$ depending on the diameter of the constriction, d, being small or large compared to ℓ [16]. The classical results correspond exactly to a quantum mechanical description of electron conduction in the adiabatic limit, which means that the degrees of freedom projected onto the aperture plane can be separated out. An electron whose trajectory passes through the constriction is assumed to traverse it like a ballistic particle without scattering. Classically, the number of possible trajectories is infinite, whereas quantization of in-plane degrees of freedom allows only a finite number of conduction channels whose conductivity is quantized in units of $2e^2/h$ [17]. For a free electron gas, the number of channels is $N_c = \pi p_F^2 d^2/h^2$ where p_F is the Fermi momentum. Expressing p_F in terms of the electron density, one obtains for the constriction conductivity

$$\sigma_c = \frac{2e^2}{h} N_c = \frac{2e^2}{h} \frac{(9\pi)^{1/3}(ZN)^{2/3}d^2}{4a^2} \quad , \tag{1}$$

where a and N denote the lattice constant and the number of atoms per unit cell, respectively, and Z is the number of valence electrons per atom. Note that by invoking Drude's theory of electron conduction, the classical expression for the constriction resistance first derived by Sharvin [18] is obtained from Eq. (1).

Thus far, $\ell \gg d$ was assumed. To obtain the conductivity of the neck in the opposite limit, one may think of the aperture as an aggregation of $N_s = d^2/(2\ell)^2$ independent subconstrictions of size $(2\ell)^2$, each comprising $\pi p_F^2 (2\ell)^2/h^2$ ballistic conduction channels. An electron that impinges on the aperture will on average probe more than one subconstriction by diffusive motion before being transmitted or reflected. Therefore, the total conductivity is equal to the ballistic conductivity of a subconstriction times the mean number of subconstrictions probed. The latter is proportional to the square root of N_s and one obtains

$$\sigma_c = \frac{2e^2}{h} \frac{(9\pi)^{1/3}(ZN)^{2/3} 2\ell d}{4a^2} \quad , \tag{2}$$

which is analogous to the classical Maxwellian conductivity. The virtue of Eq. (2) is that the close relationship between diffusive and ballistic electron transport becomes apparent. To interpolate between the two regimes, we use a simple heuristic ansatz

$$\sigma_c = \frac{2e^2}{h} \frac{(9\pi)^{1/3}(ZN)^{2/3}d^2}{4a^2} \frac{\ell}{\ell + d/2} \quad . \tag{3}$$

Hence, the normalized conductivity $\overline{\sigma}_c \equiv (h/2e^2)\sigma_c$ is equal to the number of conduction channels that are supported by the constriction multiplied by a correction factor to account for inelastic scattering effects. For $Z = 1$, which is the valence of metallic Au, the number of channels corresponds almost exactly to the number of close-packed atoms that can be accommodated in the constriction.

Owing to quantization, the conductivity (henceforth normalization is assumed) of atomic-scale contacts is predicted to change stepwise with varying contact diameter. Conductivity plateaus have indeed been observed [7–9]. However, the plateaus are generally not very distinct as a consequence of elastic scattering within the neck [9,19]. In addition, conductivities measured at plateaus frequently deviate from integer values by a substantial amount. This is in fact to be expected. According to Eq. (3), the conductivity increases on average by less than one when a channel is added, because of the finite mean free path. The effect is sizeable even for very small contacts, e.g. if we assume $\ell \approx 100$ Å, the average conductivity of a constriction consisting of 8 Au atoms is expected to be 7.5 instead of 8. Therefore, care must be exercised in inferring contact diameters from conductivity data. Neglecting mean free path effects, viz. using Eq. (1), the contact area is typically underestimated. The error increases with contact size and is expected to be less than 30% for contacts comprising fewer than, say, 100 atoms.

In the present letter, we focus on the retraction process. Nevertheless, a brief description of the indentation process is given for the sake of completeness [20]. Jump to contact is observed when the tunnel conductivity reaches a value in the range between 0.1 and 0.8. This occurs on average at a tip excursion of 10–20 Å. The initial conductivity after jump to contact is typically ≈100, indicating that a neck with a diameter of ≈30 Å had been formed (a mean area of 8 Å^2 per conduction channel is assumed). At the same time, an adhesive force due to surface tension of 10–50 nN is measured. As the indentation is continued, the adhesive force increases at first as a consequence of the thickening of the neck up to a neck diameter of ≈100 Å. From there on, compressive strain builds up, and the tip–sample force eventually becomes repulsive.

During retraction of the tip, the neck elongates by as much as 30–50 Å, and its diameter shrinks to atomic dimensions before breaking. The latter is a clear sign of plastic deformation. Eventually, tunneling is observed after the neck breaks, which proves that only very little elastic strain is present. A set of force and conductivity data measured during retraction of the tip is shown in Fig. 2. This example was selected because atomic-scale features can be particularly clearly seen. We would like to emphasize, however, that the trends to be described below are generally valid. In the first phase, the neck diameter is frequently observed to grow slightly as the compressive stress is released. In the next phase, tensile stress is built up in the neck, whose diameter remains approximately constant. Thinning and elongation of the neck sets in somewhat abruptly when the tensile stress exceeds a critical value of ≈6 GPa, irrespective of the contact diameter and previous loading forces. The process evolves discontinuously as is evidenced by the characteristic oscillation of the tip-sample force which correlates with the step structure of the conductivity. The average tensile stress, however, remains approximately at the critical value during the entire elongation process. Evidently, these nanometer-sized contacts are substantially more rigid than their macroscopic counterparts, which yield at a tensile stress of typically 150 MPa.

The overall dependence of the contact area versus tip–sample distance, s, is discussed next. MD simulations suggest that plastic deformation occurs locally within a few atomic layers adjacent to the constriction. Hence, a mass balance equation $nd_0\Delta A_c = \Delta s A_c$ can be written, where A_c is the contact area, n is the number of atomic layers involved in the deformation process, and d_0 is their spacing. The contact area is thus predicted to decrease exponentially with s with a decay constant of $1/nd_0$. Alternative to the local picture, one can view the necking process as a sequence of shear relaxations. They are initiated by slip dislocations at the constriction which propagate along glide planes. In each such step, the contact area shrinks in proportion to the contact diameter, $\Delta A_c = \lambda \Delta s A_c^{1/2}$, where the proportionality factor λ is of the order of unity. Hence, one expects a parabolic dependence of the contact area on s. To check the model predictions against our data, we plotted the logarithm and the square root of the conductivity versus s. Deviations of the plots from a straight line indicate inadequacies of the respective model. The experimental data falls between the two limiting cases, with the overall rate of change of the contact area predicted to be too large and too small for the local disorder and shear model, respectively.

The conductivity versus distance curve shows remarkably well-developed plateaus, which are particularly pronounced when the number of atoms in the constriction is less than $\approx$10. Note, however, that the conductivity of some of the plateaus deviates significantly from integer values. An analysis of more than 300 indentation experiments revealed that for $\overline{\sigma}_c \leq 6$, the correlation with integer values was statistically significant, whereas for $\overline{\sigma}_c \geq 10$, no such correlation could be established. This is not surprising because the mean free path is certainly not larger than 100 Å. The most remarkable feature of the data is the almost perfect correlation between local maxima of the adhesive tip–sample force with corner points of the conductivity plateaus. This unambiguously proves that the conductivity plateaus are intimately connected with the atomic structure in the neck.

To shed some light on the atomistic processes involved, we compare our results with MD predictions [11]. Two important qualitative differences can be identified. First, the amplitude of the force oscillations is basically constant in the experiment, whereas it increases rougly proportional to the contact size in the simulation. Second, in the MD simulations the maximum of the adhesive force corresponds to a maximum of elastic strain just before the neck yields. The latter entails rearrangement of atoms such that a new layer is added to the neck and, accordingly, the constriction diameter shrinks. Hence, when the tip is retracted, the maximum of the adhesive force is predicted to be followed by a sudden drop of the conductivity, whereas experimentally the opposite sequence is observed. Therefore, we conclude that plastic deformation of these Au contacts proceeds qualitatively in a different way.

There is a natural explanation for our experimental observations if we take shear relaxation as the principal deformation mechanism. Here, the crystalline order is basically preserved. Relaxation is initiated by the nucleation of a slip dislocation at the edge of the constriction, where tensile stress is maximum. The nucleation of a slip dislocation involves breaking atomic bonds and their subsequent exposure to vacuum. Hence, the nucleation corresponds to a maximum of the adhesive force. Simultaneously, the cross section of the constriction shrinks by the number of bonds broken, which in turn gives rise to a corresponding decrease of the conductivity. As the tip is retracted farther, the slip dislocation propagates along a glide plane most likely within the tip which, however, has little effect on the contact area. Therefore, this model predicts that a rapid change of the conductivity will coincide with a rapid increase of the adhesive force, in line with experimental observation. Furthermore, the activation energy deduced from integrating the force versus distance curve is of the order of 2 eV. This value is approximately equal to the surface free energy of an area equivalent to the average number of conduction channels lost in one deformation step. We are aware that this simplistic model cannot completely account for all experimental facts. In particular, the contact area versus distance characteristics suggest that other relaxation mechanisms involving disorder and diffusion of point defects are also important.

In conclusion, we have performed a classic indentation experiment to study plastic deformation of atomic-sized Au contacts. The experimental results, which contradict MD predictions, show that our understanding of the atomistic processes involved is still incomplete. From the analysis of our data, we conclude that nucleation of slip dislocations and subsequent shear are the dominant processes by which these Au contacts deform.

ACKNOWLEDGMENTS

We would like to thank E. Delamarche for preparing the Au samples. We gratefully acknowledge fruitful discussions with J. Pethica, U. Landman, J. Israelachvili, F. Besenbacher and J.K. Nørskov. One of us (A.S.) thanks the University of Fribourg (Switzerland) for financial support.

[1] S.K. Roy Chowdhury and H.M. Pollock, Wear **66**, 307 (1981).

[2] H.M. Pollock, P. Shufflebottom, and J. Skinner, J. Phys. D: Appl. Phys. **10**, 127 (1977).

[3] M.D. Pashley, J.B. Pethica, and D. Tabor, Wear **100**, 7 (1984); M.D. Pashley, J.B. Pethica, J. Vac. Sci. Technol. A**3**, 757 (1985).

[4] J.K. Gimzewski and R. Möller, Phys. Rev. B **36**, 1284 (1987).
[5] N.A. Burnham and R.J. Colton, J. Vac. Sci. Technol. A **7**, 2906 (1989).
[6] S.R. Cohen, G. Neubauer, and G.M. McClelland, J. Vac. Sci. Technol. A**8**, 3449 (1990).
[7] J.I. Pascual, J. Méndez, J. Gómez-Herrero, A.M. Baró, N. García, and Vu Thien Binh, Phys. Rev. Lett. **71**, 1852 (1993).
[8] J.M. Krans and C.J. Muller, Phys. Rev. B **48**, 14721 (1993) .
[9] L. Olesen, E. Lægsgaard, I. Stensgaard, F. Besenbacher, J. Schiøtz, P. Stoltze, K.W. Jacobsen, and J.K. Nørskov, Phys. Rev. Lett. **72**, 2251 (1994). Proc. R. Soc.
[10] U. Landman, W.D. Luedtke, N.A. Burnham, and R.J. Colton, Science **248**, 454 (1990).
[11] U. Landman, W.D. Luedtke, and E. Ringer, Wear **153**, 3 (1992).
[12] T.N. Todorov and A.P. Sutton, Phys. Rev. Lett. **70**, 2138 (1993).
[13] R.M. Lynden-Bell, Science **263**, 1704 (1994).
[14] A. Stalder and U. Dürig, in: Proceedings of the NATO Advanced Study Institute on "Forces in Scanning Probe Methods," March 7-18, 1994, Schluchsee, Germany, NATO ASI series E: Applied Sciences (Kluwer, Dordrecht, in press).
[15] U. Dürig, O. Züger, and A. Stalder, J. Appl. Phys. **72**, 1778 (1992).
[16] See e.g. A.G.M. Jansen, A.P. van Gelder, and P. Wyder, J. Phys. C: Solid St. Phys. **13**, 6073 (1980).
[17] M. Büttiker, Y. Imry, R. Landauer, and S. Pinhas, Phys. Rev. B **31**, 6207 (1985); R. Landauer, Z. Phys. B–Condensed Matter **68**, 217 (1987).
[18] Y.V. Sharvin, JETP **48**, 984 (1965).
[19] E. Tekman and S. Ciraci, Phys. Rev. B **43**, 7145 (1991).
[20] A detailed report on indentation experiments is in preparation.

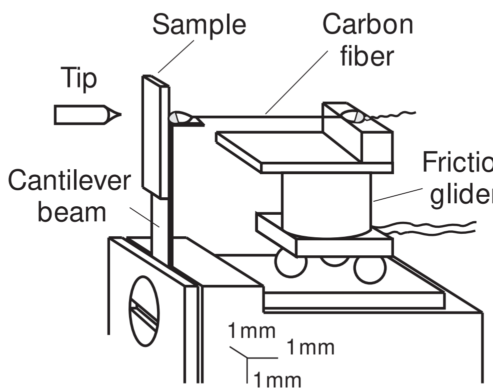

FIG. 1. Schematic diagram of the force sensor. From [14].

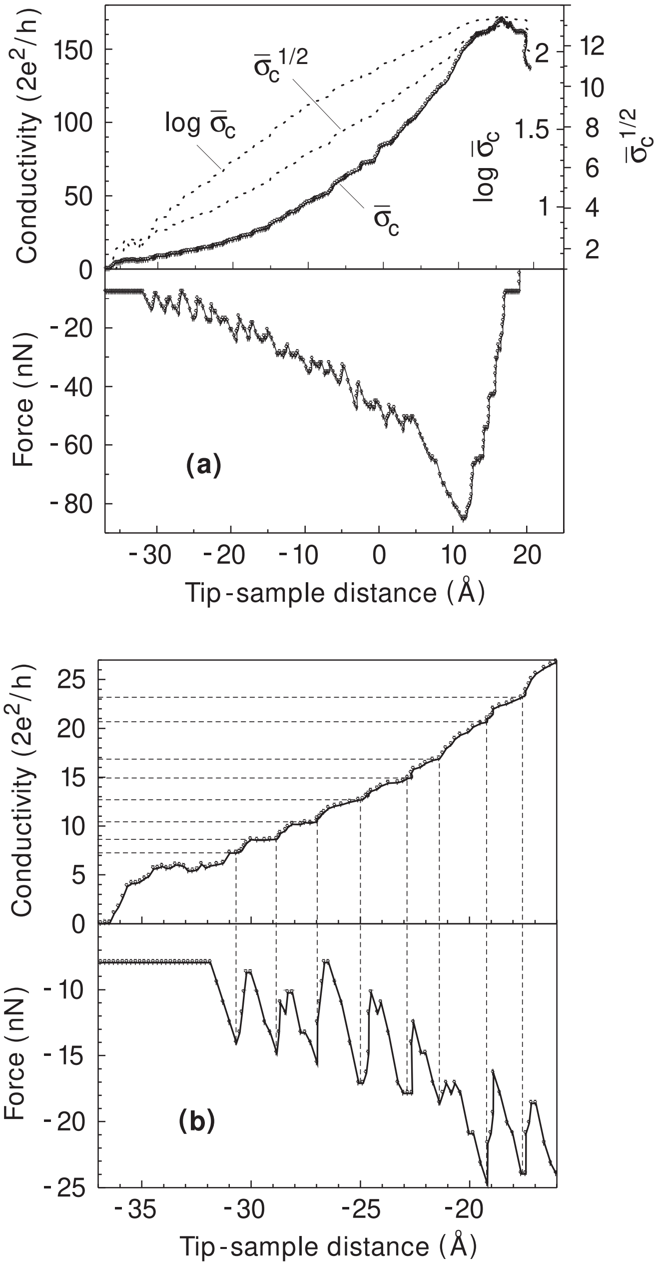

FIG. 2. (a) Conductivity and tip–sample force measured while the tip is being retracted from the surface after indentation. (b) Same as (a), but showing the last phase of contact necking on an expanded scale (force data for $s < -32$ Å is corrupted by a malfunctioning of the sensor).